This is the accepted version of the following article: Murza, A., Parent, A., Besserer-Offroy, E., Tremblay, H., Karadereye, F., Beaudet, N., Leduc, R., Sarret, P. and Marsault, É. (2012), Elucidation of the Structure–Activity Relationships of Apelin: Influence of Unnatural Amino Acids on Binding, Signaling, and Plasma Stability. ChemMedChem, 7: 318–325. doi: 10.1002/cmdc.201100492, **which has been published in final form at** http://onlinelibrary.wiley.com/doi/10.1002/cmdc.201100492/abstract

Elucidation of the structure/activity relationships of apelin: influence of unnatural amino acids on binding, signaling and plasma stability

Alexandre Murza,[a,b] Alexandre Parent,[b] Elie Besserer-Offroy,[a,b] Hugo Tremblay,[a] Félix Karadereye,[a] Nicolas Beaudet,[b] Richard Leduc,[a] Philippe Sarret,[b] Eric Marsault [a],*

[a]*Département de pharmacologie,* [b]*Département de physiologie et biophysique, Faculté de médecine et des sciences de la santé, Université de Sherbrooke, Sherbrooke, QC, Canada*

ABSTRACT

Apelin is the endogenous ligand of the APJ receptor, a member of the G protein-coupled receptor family. The apelin/APJ complex has been detected in many tissues and is emerging as a promising target for a number of pathophysiological conditions. There is currently little information on the structure/activity relationship (SAR) of the apelin hormone. In an effort to better delineate SAR, we synthesized analogs of apelin-13 modified at selected positions with unnatural amino acids, with a particular emphasis on the C-terminal portion. Analogs were then tested in binding and functional assays by evaluating $G_{i/o}$ mediated reduction in cAMP levels and by assessing β-arrestin2 recruitment to the receptor. The plasma stability of new analogs was also assessed. Several were found to possess increased binding and higher stability compared to the parent peptide.

KEYWORDS

Apelin, APJ, Structure/activity relationship, GPCR, plasma stability, downstream signaling

TABLE OF CONTENTS

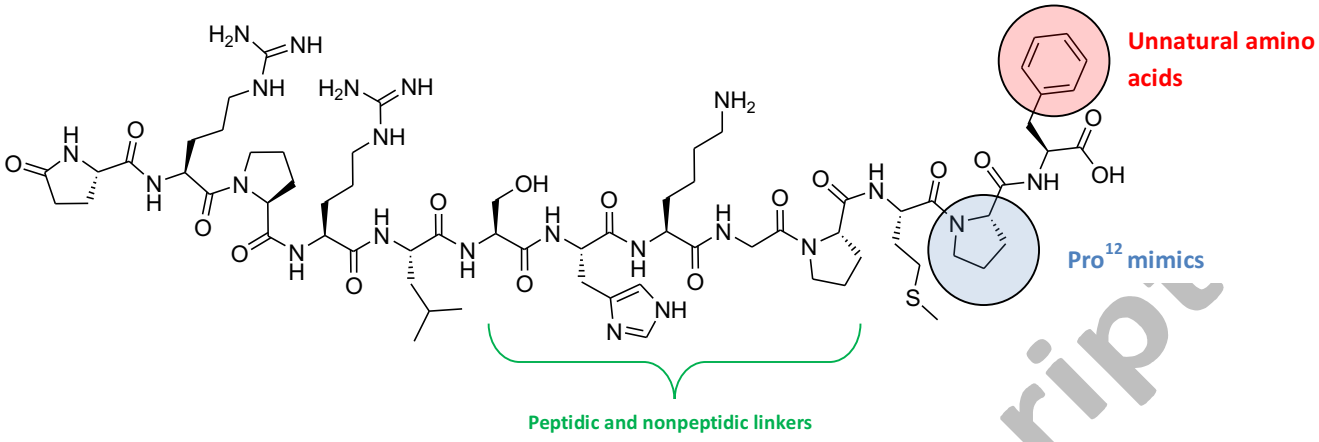

The SAR of apelin-13 with the APJ receptor was evaluated by D-scan, replacement of Phe^{13} and Pro^{12} and the central portion with selected unnatural amino acids. The activity of analogs was tested in binding and functional assays on the G_i and β-arrestin2 pathways, and their stability in plasma assessed.

INTRODUCTION

The apelin receptor (angiotensin receptor like-1; APJ) was cloned in 1993 [1] and later deorphanized when its endogenous ligand, apelin, was isolated from bovine stomach extracts by Tatemoto *et al.* [2]. The apelin/APJ system has since been detected in many peripheral tissues such as heart, kidney, pancreas and lungs, as well as in the central nervous system, suggesting diverse roles in human physiology [3-14]. In the past decade, several studies have confirmed the involvement of apelin peptides in various normal and pathological conditions, including cardiovascular, metabolic, gastrointestinal diseases, tumor angiogenesis, hypoxia, and HIV infection [15-24]. The pathophysiological roles and potential applications of the apelin/APJ system are the subject of a growing body of literature and were reviewed recently [25].

The APJ receptor belongs to the rhodopsin-like G protein-coupled receptor (GPCR) family and shares a high homology with the angiotensin 1 receptor (AT1R) [1]. Activation of the apelin receptor triggers intracellular signaling pathways through $G_{i/o}$- and G_q-mediated coupling [26, 27], leading to the reduction of cAMP production, release of internal calcium stores, and activation of mitogen-activated protein-kinases (ERK1/2) and phospholipase C [28, 29]. The activated APJ receptor also recruits both β-arrestin1 and β-arrestin2 and internalizes through different trafficking routes [30].

Following proteolysis, apelin peptides of different lengths are produced, of which apelin-36, -17, -13 (or its pyroglutamate analog Pyr^1-apelin-13 **[Figure 1]**) are the most predominant; these different forms have been investigated in several contexts. In terms of structure, Langelaan *et al.* [31] thoroughly studied the solution conformations of apelin-17 and demonstrated that the peptide does not possess α-helical or β-sheet secondary structure as revealed by circular dichroism (CD) spectroscopy. They also reported that the Arg^2-Pro^3-Arg^4-Leu^5 segment adopts a more ordered structure as shown by two-dimensional nuclear magnetic resonance spectroscopy (2D NMR) [31]. This observation and that from the alanine scan (see below) was exploited by Macaluso *et al.* and by Hamada *et al.* to design macrocyclic APJ agonists and antagonists [32-34]. In terms of Structure-Activity Relationships (SAR), Medhurst *et al.* reported a detailed alanine scan performed on Pyr^1-apelin-13 [26], pinpointing key residues involved in APJ receptor binding (Pyr^1-apelin-13: Pyr^1-Arg^2-Pro^3-Arg^4-Leu^5-Ser^6-His^7-Lys^8-Gly^9-Pro^{10}-Met^{11}-Pro^{12}-Phe^{13}) and in activation of the $G_{i/o}$ pathway. Indeed, substitutions of Arg^2 and Leu^5 were shown to lead to a 1.7 log decrease in binding and second messenger coupling [23, 26], consistent with a role as potential pharmacophoric residues.

This is also in agreement with the higher level of order of this segment of the peptide [31]. Additionally, truncation of the N-terminal end resulted in a marked decrease in both affinity and efficacy, in agreement with the pharmacophore model proposed by Itturioz *et al.* who recently reported the first non-peptidic APJ agonist E339-3D6 (IC_{50} 430 nM) [35]. This molecule, which contains a tricationic moiety coupled to a polyaromatic fluorophore through a flexible hydrophobic spacer, is thought to interact with the APJ receptor via two distant epitopes. On the one hand, these interactions involve cationic residues Arg^2 and Arg^4 in the N-terminal of the peptide (Arg^2-Pro^3-Arg^4-Leu^5) and residues Asp^{184} and Asp^{282} of the APJ receptor, and on the other hand a hydrophobic, π-stacking type interaction between the C-terminal Phe^{13} residue and a polyaromatic pocket deep in the transmembrane domain involving residues Trp^{152}, Trp^{259} and Phe^{255} of the APJ receptor [36]. Finally, apelin is hydrolyzed by the angiotensin-converting enzyme 2 (ACE-2), which cleaves the peptide between residues Pro^{12} and Phe^{13}, resulting in a half-life inferior to 1 min [37].

Based on these observations, our aim was to better delineate Structure-Activity Relationships (SAR) of apelin and the APJ receptor with respect to binding and functional efficacy on the $G_{i/o}$- and the β-arrestin2 signaling pathways. Toward this end, we first performed a (D)-scan on every position, then focused on the C-terminal segment by replacing selected residues by unnatural amino acids. Modifications to the central portion of the peptide were also performed with nonpeptidic residues. Finally, plasma stability of the new synthesized analogs was assessed.

RESULTS AND DISCUSSION

D-scan

In order to better understand the role of each residue of apelin-13 and as a complement to the reported alanine scan data [26], we performed a systematic replacement of each residue by its D-isomer **[Table 1]**. Every compound was tested in a 7-point curve radioligand binding assay to determine its IC_{50} value, and in a cyclic adenosine monophosphate (cAMP) accumulation assay at a single concentration of 10 μM to confirm its agonist activity. First, single substitution of Pro^{12}, Met^{11}, Leu^{5} and Pyr^{1} by their D-analogs (**3**, **4**, **9,** and **13**, respectively) resulted in mild decrease in binding compared to the native peptide Pyr^{1}-apelin-13 (**Ape13**). These results suggest that the residue Pro^{12} is likely not critical to impose rigidity on the C-terminal end of the peptide. While results on Met^{11} and Pyr^{1} confirm their limited role for receptor interaction as previously reported with the Ala scan [26], inversion of configuration on residues Leu^{5} and Phe^{13} led to a modest decrease in binding (**9** and **2**, IC_{50} 61 and 109 nM, respectively) compared to Pyr^{1}-apelin-13 (IC_{50} 5.7 nM). In contrast, inversion of configuration on the central amino acids Ser^{6}, His^{7} and Lys^{8} induced a significant 50- to 100-fold decrease in binding (analogs **6, 7, 8**). These results, which contrast with those of the Ala scan [26], suggest that although side chains of Ser^{6}-His^{7}-Lys^{8} may not interact directly with the receptor, inversion of their configuration possibly changes the basal conformation of the peptide and imposes a rearrangement of the skeletton upon binding, accompanied by a significant entropic penalty [38]. Unlike Pro^{12}, the inversion of configuration of Pro^{10} decreased binding by more than 2 orders of magnitude (**5**, IC_{50} 1.6 μM), suggesting a role in structuring the peptide. We also observed an important loss of affinity for (D)Pro^{3} analog **11**, suggesting a critical role in structuring the chain [31]. Finally, as expected, inversion of configuration of Arg^{4} and Arg^{2} impaired binding dramatically (**10** and **12**; IC_{50} 1.3 and 4.1 μM, respectively), with a greater impact on Arg^{2}, consistent with the Ala scan [26]. Similar to Pyr^{1}-apelin-13, all of these new apelin analogs behaved as full agonists at APJ receptors ($G_{i/o}$ pathway), inhibiting forskolin-induced cAMP accumulation by 85-95 % at a single concentration of 10 μM.

C-terminal substitutions

The C-terminal Phe^{13} of apelin-13 appears to have a pivotal role in the SAR with the APJ receptor. Indeed, truncation or replacement by Ala of the C-terminal Phe residue yields a peptide able to modify the properties of receptor internalization [36, 39]. Furthermore, the Ala scan [26] or the D-scan reported here demonstrated that deletion or substitution of Phe^{13} leads to approximately a 10-fold decrease in binding and functional efficacy ($G_{i/o}$ pathway). With this in mind, we replaced Phe^{13} by unnatural amino acids to further explore SAR locally **[Table 2, Figure 2]**. This set of modifications was performed on the Met11Nle analog to circumvent oxidation side products frequently associated with the presence of Met in peptides [40]. The Met11Nle analog (**1**, IC_{50} 2.6 nM) possesses a similar profile in terms of affinity, coupling to second messenger cascades, and stability to that of Pyr^{1}-apelin-13 (IC_{50} 5.7 nM).

Aromatic interactions have been proposed as critical determinants of receptor internalization [36]. This observation has direct consequences on the physiological activity of APJ and other GPCRs [39]. Given the proposal that several aromatic residues interact with the terminal Phe of apelin-13 (Trp^{152}, Trp^{259} and Phe^{255}) in the transmembrane domain [36], Phe^{13} was replaced by the unnatural amino acids, diphenylalanine (Dip) and biphenylalanine (Bip), which possess increased capacity for π-π interactions and could be used to probe the binding pocket. Phe13Dip (**14**, IC_{50} 88 nM) and Phe13Bip (**15**, IC_{50} 7.8 nM) display a 10-fold difference in affinity. Given the rigid positioning of aromatic groups on these unnatural amino acids, these results suggest that the C-terminal binding site is deep rather than wide. Interestingly, Phe13Cha (**18**, IC_{50} 2.3 nM) possesses an affinity comparable to that of Pyr^{1}-apelin-13, indicating that hydrophobic interactions are necessary for binding, but aromatic, π-stacking type interactions are not essential.

Accordingly, Phe13-1Nal (**16**, IC_{50} 14.1 nM) and Phe13-2Nal (**17**, IC_{50} 1.2 nM) showed a 10-fold difference in favor of the 2Nal analog. The similarity with Phe13Trp (**19,** IC_{50} 8.5 nM) suggests that additional H-bonding and/or increased electron density [41] could be detrimental for affinity. The result with 1Nal is consistent with that of Phe13Trp, since 1Nal is considered a bioisosteric replacement for Trp [42]. On the other hand, electron-poor analogs (4-Br)Phe **20**; (2,4,5-trifluoro)Phe **21** and (4-nitro)Phe **22** all demonstrated improved binding compared to Phe, particularly **21** which possesses sub-nM affinity (0.8 nM). Altogether, the above results suggest that, despite not being a prerequisite, there is a possibility of π-stacking interaction with electron-

rich residues [36] in the binding pocket of APJ, which is more favorable with electron-poor residues on apelin (to be noted the (2,4,5-trifluoro)Phe is the poorest of the aforementioned [43]).

All C-terminal analogs showed similar agonist profiles (EC_{50} 10-20 nM) in the cAMP accumulation assay when compared to Pyr^1-apelin-13 (EC_{50} 1.9 nM), except for Phe13Trp (**19**, 58.5% inhibition). In the β-arrestin2 assay, we observed an interesting trend between Phe13-1Nal (**16**, EC_{50} 522 nM) and Phe13-2Nal (**17**, EC_{50} 70 nM), showing the possibility of a particular C-terminal pocket occupation for β-arrestin2 activation. Consistently with the binding assay, electron-poor analogs **20** (EC_{50} 28 nM**), 21** (EC_{50} 32 nM) and **22** (EC_{50} 53 nM) provided higher efficacy in the β-arrestin2 assay compared to Pyr^1-apelin-13 (EC_{50} 91 nM). Altogether, these results reinforce previous findings [36, 39] indicating the implication of the C-terminal residue in APJ receptor internalization. The stability of the newly synthesized analogs was further evaluated *in vitro* in rat plasma and compared to that of Pyr^1-apelin-13. In general, C-terminal substitutions provided significant improvements in plasma stability especially for analogs presenting increased steric hindrance (analogs **14**, **15**, **16**, **17**).

Pro^{12} substitutions

Apelin-13 stability is low in human plasma ($t_{1/2}$ ~ 1 min) [37]. The critical step in apelin stability *in vivo* has been attributed to hydrolysis by the angiotensin-converting-enzyme 2, which cleaves the hormone between residues Pro^{12} and Phe^{13} [37]. Thus, in order to both better understand SAR and potentially improve plasma stability, we synthesized several analogs in which Pro^{12} was replaced by unnatural amino acids providing different steric or conformational environment **[Table 3, Figure 3).**

Replacement of Pro^{12} by aminoindane (**27**, IC_{50} 20 nM) and Tle (**31**, IC_{50} 15.6 nM) mildly decreased affinity, possibly due to changes in local conformation. Surprisingly, replacement of Pro^{12} by the γ-amino isonipecotic acid (**30**, IC_{50} 5.0 nM) did not affect affinity. Importantly, replacement of Pro^{12} by Aib (aminoisobutyric acid (**24, 29**)) provided a very potent analog, with an IC_{50} of 0.76 nM, almost 10-fold better than Pyr^1-apelin-13. The absence of substantial impacts on affinity suggests that substitution of Pro^{12} with unnatural residues or D-analogs is not critical for positioning the terminal Phe residue. However, combination of the $2Nal^{13}$ and Aib^{12} modifications did not provide the expected synergy in terms of affinity (**32**, IC_{50} 3.6 nM). Deletion

of the Pyr^1Arg^2 (**33**, IC_{50} 2928 nM) and $Pyr^1Arg^2Pro^3$ (**34**, IC_{50} 3453 nM) segments altogether was very detrimental to binding. However, all these truncated analogs preserved their agonist profile on the $G_{i/0}$ pathway (~ 90% cAMP inhibition) but not on the β-arrestin2 pathway (>3000 nM), suggesting that the distance between the two epitopes may be important for receptor endocytosis and trafficking. As a matter of fact, the apelin-13 internalized receptor is rapidly recycled to the cell surface, whereas the apelin-36 internalized receptor is addressed to intracellular compartment [30]. Others analogs of this series kept their agonist profile, with less than 10-fold difference compared to Pyr^1-apelin-13, except for Pro12aminoindane (**27**, 53.3 % cAMP inhibition, EC_{50} β-arr2 1.2 μM). Surprisingly, Pro^{12} substitutions generally did not increase stability (**24** vs **30**). Analog **24**, which possesses a 10-fold increased affinity, is also significantly more stable in plasma than Pyr^1-apelin-13. Again, the combination of $2Nal^{13}$ and Aib^{12} (**32**) substitution affected stability. Pro12cycloleucine **28** and truncated analogs **33**, **34** were completely degraded after 1 h.

Modifications to the central portion of the peptide

Both alanine- and D-scan data suggest that the Arg^2-Pro^3-Arg^4-Leu^5 portion of apelin is important for binding to the APJ receptor [26]. In contrast, replacement of Ser^6, His^7 or Lys^8 by Ala had very little effect on binding [26]. Additionally, NMR and CD data suggest that the central segment of apelin is both less critical for receptor interactions and less conformationally restricted [31]. In agreement with this, the pharmacophore model proposed by Iturrioz *et al.* [35] suggests a two-epitope model connected by a flexible linker and involving the N-terminal Arg^2-Pro^3-Arg^4-Leu^5, the Phe and carboxylate C-terminal [35, 36]. These data suggest that the central portion of the peptide is less critical for receptor interactions, however details of interaction remain to be elucidated. To investigate this further, we replaced it by a flexible and hydrophilic polyethylene glycol (PEG) linker, or by a more rigid, helix-inducing poly(alanine) fragment [44]. Accordingly, we synthesized analogs with PEG_6, PEG_4, $(Ala)_4$ as well as a truncated analog devoid of residues 6 to 9 **[Table 4]**. The four analogs were associated with important reductions in affinity. It has been previously described [32] that a hydrogen bond is formed between Ser^6 side chain and the Leu^5 backbone carbonyl, stabilizing the Arg^4-Leu^5-Ser^6-His^7 β-turn, which is absent in the four analogs and could partially explain the drop in affinity. For PEG_4 (**35**, IC_{50} 450 nM) and PEG_6 (**36**, IC_{50} 13.7 μM) analogs, affinity decreased by 80- and more than 2000-fold respectively, whereas replacement of the central segment by $(Ala)_4$ (**38**, IC_{50} 3.7 μM) led to a 500-fold decrease in affinity. The fact that

the PEG_4 analog possessed higher affinity compared to the $(Ala)_4$ analog suggests that a flexible backbone is preferable, independently of direct molecular interactions with the receptor. Indeed, poly(alanine) are known to induce helical conformations [44]. Surprisingly, truncation of the central four amino acids did not result in complete loss of affinity (**37**, IC_{50} = 5.4 μM). However, it underlines the importance of the two epitopes of the peptide for binding, in agreement with the proposed pharmacophore model [35].

Functionally, this latter series of analogs was not very efficacious at activating the G_i pathway. Indeed, **35** – **38** inhibited cAMP accumulation by only 10-22% at 10 μM. These analogs seem to behave as antagonists, which will be further investigated. Analogs with modifications to the central portion (**35**, **36**, **37**, **38**) possessed improved plasma stability, possibly due to changes in conformation and replacement of peptidic backbones by PEGs.

Conclusion

In conclusion, this study refines existing SAR of the apelin hormone and opens interesting avenues for future work. It demonstrates that the spatial orientation of some residues of the apelin peptide is important, despite little effect in the alanine scan. It also underlines the critical importance of Arg^2, Pro^3, Arg^4 and the lesser role of Pro^{12}. With the help of selected unnatural amino acids, we also studied SAR on the C-terminal end of the peptide via binding and agonist profiling on two pathways ($G_{i/o}$, β-arrestin2), by substituting Phe^{13} with different types of aromatics. It led to better delineation of the shape of the C-terminal pocket, demonstrating the possibility of hydrophobic, non-aromatic interactions, and confirming the interaction of the C-terminal Phe with electron-rich residues in the binding pocket of the APJ receptor. Central amino acids were also substituted by various linkers (PEGs, Alanine), demonstrating the importance of distance and rigidity between the two epitopes. Substitutions of Pro^{12} with amino acids inducing variable steric hindrance were generally well tolerated. The plasma stability of new analogs was assessed. C-terminally and centrally modified analogs showed significant improvements plasma stability compared to Ape13, whereas analogs modified at Pro^{12} displayed more variable results. This study also reports a series of peptide agonists of the APJ receptor with higher affinity and plasma stability than Pyr^1-apelin-13. It opens a number of new avenues, which are under investigation and will be reported in due course.

ACKNOWLEDGMENTS

Financial support from Université de Sherbrooke, the Natural Sciences and Engineering Research Council of Canada (Collaborative Research & Development Grant with Tranzyme Pharma) and Tranzyme Pharma Inc. is gratefully acknowledged. Institut de Pharmacologie de Sherbrooke (IPS) is also acknowledged for scholarship to A.M. and E.B.-O. P.S. is the recipient of an FRSQ Junior 2 salary support. Pr G. Guillemette and L. Gendron are gratefully acknowledged for providing lab space and equipment for biological assays.

MATERIALS AND METHODS

Procedures for solid phase synthesis

Materials

Protected amino acids, TentaGel S PHB Phe Fmoc resin and TentaGel S PHB, O-[4-(Hydroxymethly)phenyl]polyethylene glycol resin were purchased from ChemImpex International (USA) and Rapp Polymere (Germany). All other reagents were purchased from Sigma-Aldrich (Canada), Fisher Scientific (USA) or ACP (Canada) and were of the highest commercially available purity. Peptide synthesis was performed in 12 mL polypropylene cartridge with 20µ PE frit from Applied Separations (USA).

Analogs with phenylalanine as C-terminal amino acid

Tentagel S PHB Phe Fmoc resin (0.25 mmol/g, 0.3 g) was treated with 20% piperidine/DMF (*N,N*-dimethylformamide) during 30 min and reacted with a Fmoc N-protected amino acid (5 equiv.) in the presence of [O-(7-azabenzotriazol-1-yl)-1,1,3,3-tetramethyluronium hexafluorophosphate] HATU (5 equiv.), *N,N*-diisopropylethylamine (10 equiv.) in DMF (4 mL). The coupling reaction time was 1 h at room temperature (generally sufficient to obtain complete coupling as judged by the Kaiser test [45]) and piperidine (20% in DMF) was used to cleave the Fmoc group at every step. The resin was washed after each coupling step and deprotection by shaking 5 min in DMF (2x 5 mL), 2-propanol (1x 5 mL), DCM (1x 5 mL), 2-propanol (1x 5 mL), DCM (1x 5 mL), DMF (2x 5 mL). For resin cleavage, the resin was treated with a mixture of TFA (trifluoroacetic acid)/H_2O/TIPS (Triisopropylsilane), 95/5/5, v/v] (4 mL / 0.3 g of resin) for 4 h at room temperature. After filtration of the resin, peptide was precipitated in TBME (*Tert*-butyl methyl ether) at 0°C, the suspension was centrifuged, the supernatant was removed and the crude product was redissolved in water then lyophilized. Purification by reverse-phase chromatography (described below) yielded the desire products as white powders after lyophilization.

Analogs with a different C-terminal amino acid that phenylalanine

Coupling of the terminal amino acid to the resin, TentaGel S PHB, O-[4-(Hydroxymethly)phenyl]polyethylene glycol resin (0.27 mmol/g, 0.3 g) was treated with triphenylphosphine (7.4 equiv.), diisopropyl azodicarboxylate (DIAD, 7.4 equiv.), Fmoc protected amino acid (7.4 equiv.) and tetrahydrofuran (THF, 4 mL) as solvent. The reaction was run overnight at room temperature, then the resin was washed for 5 min with DCM (2x 5 mL), toluene (1x 5 mL), EtOH (1x 5 mL), toluene (1x 5 mL), DCM/MeOH (75/25, 1x 5 mL), THF/MeOH (75/25, 1x 5 mL), DCM/MeOH (75/25, 1x 5 mL), THF/MeOH (75/25, 1x 5 mL), DCM (2x 5 mL). The resin was then treated with DCM/Ac_2O/DIPEA (20/5/1, v/v/v, 5 mL) at room temperature during 1h, and washed with DCM (3x 5 mL), DCM/MeOH (75/25, 5 mL), DCM (3x 5 mL). The rest of the synthesis was pursued as indicated above.

Peptide purification and characterization

Crude peptides were purified by reverse-phase chromatography using an ISCO CombiFlash Sq16x system with a Silicycle C_{18} column (12 g, 60 A, 40-63 µm spherical particle size column) and a linear gradient of 5-30% acetonitrile in water containing 0.1% TFA over 60 min. Analytical HPLC analyses were performed on an Agilent 1100 series equipped with UV detector set at 223 nm and an Agilent Eclipse Plus C_{18} column (3.0 x 50 mm, 1.8 µm spherical particle size column). The gradient was 2-50% acetonitrile in water containing 0.1% TFA (10 min), 50-100% (4 min), 100% (4 min), 100-2% (1 min) and 2% (3 min). Most analogs possessed UV purity >95% at 223 nM. Molecular weights of compounds were determined by mass spectrometry (Electrospray micromass ZQ-2000 from Waters).

Binding and cAMP accumulation assays

Materials

High glucose Dulbecco's Modification of Eagle's Medium (DMEM), G418 and penicillin/streptomycin were purchased from Invitrogen Life Technologies (Canada). Fetal bovine serum (FBS) and Hank's balanced saline solution (HBSS) were purchased from Wisent (Canada). 4-(2-hydroxyethyl)-1-piperazineethanesulfonic acid (HEPES), potassium chloride (KCl), calcium

chloride ($CaCl_2$), magnesium chloride ($MgCl_2$), ethylene glycol tetraacetic acid (EGTA), glucose, sodium bicarbonate ($NaHCO_3$), sodium hydroxide (NaOH) and bovine serum albumin (BSA) were purchased from BioShop (Canada). Adenosine 3',5'-cyclic monophosphate (cAMP), adenosine 5'-triphosphate disodium salt hydrate (ATP), 3-isobutyl-1-methylxanthine (IBMX), imidazole and forskolin were purchased from Sigma-Aldrich (Canada). Sodium chloride (NaCl) and trichloroacetic acid (TCA) were purchased from Fisher Scientific (Canada). Hydrochloric acid (HCl) was purchased from Anachemia Science (Canada). [^{3}H]-adenine and [^{125}I]-apelin13 were purchased from PerkinElmer (Canada). Polyethylenimine (branched PEI) was obtained from Polysciences (USA). Coelenterazine-400A (DeepBlueC) was purchased from Biosynth International Inc. (USA). White opaque 96-well half area plates were obtained from Perkin Elmer (Canada). BRET2 measurements were performed on an M1000 plate reader from Tecan (USA).

Cell culture

Stable cell lines expressing the YFP epitope-tagged human APJ receptor (HEK 293 cells) were cultured in high glucose Dulbecco's Modification of Eagle's Medium (DMEM), supplemented with 10% fetal bovine serum (FBS). Cells were kept in a humidified atmosphere with 5% CO_2 at 37^{o}C according to the manufacturer's instructions. Three to four days before the assay, cells were plated in 35 mm culture dishes and used at 80% confluence. G418 and penicillin/streptomycin were used as selection agent and antibiotics, respectively.

Membrane preparation

Binding experiments were carried out on freshly prepared membrane homogenates. Briefly, 24 h after plating confluent HEK-293 cells were scraped off the culture dishes with 50 mM ice-cold Tris-HCl buffer, pH 7.5. Subsequently, the cells were centrifuged at 13000 rpm for 5 min at 4°C in microcentrifuge tubes and resuspended in hypotonic TE buffer (5 mM EDTA and 10 mM Tris-HCl, pH 7.5). Membrane homogenates were then sonicated, recentrifuged at 13000 rpm for 30 min at 4°C and finally resuspended in the same TE buffer.

Radioligand binding experiments

Competition radioligand binding experiments were performed by incubating cell membranes (50 µg) with 0.2 nM [^{125}I]-Apelin-13 (2200 ci/mmol) and increasing concentrations of various apelin analogs (10^{-11} to 10^{-5} M) for 30 min at 25°C in 250 µL binding buffer (50 mM Tris-HCl buffer, pH 7.5, containing 0.2% bovine serum albumin). Incubations were terminated by addition of 2 mL ice-cold binding buffer followed by filtration through glass microfiber filters (GF/C, Whatman) pre-incubated overnight with 0.5% polyethylenimine in binding buffer. After washing twice with 2 mL ice-cold binding buffer, the radioactivity retained on the filter was counted in a γ-counter 1470 Wizard form Perkin Elmer (75% counting efficiency). Nonspecific binding was measured in the presence of 10^{-5} M unlabeled Pyr^{1}-apelin-13 and represented less than 5% of total binding. IC_{50} values were determined from inhibition curves as the unlabeled ligand concentration inhibiting 50% of [^{125}I]-Apelin13 specific binding. All binding data were calculated and plotted using Graphpad Prism 5 and represent the mean ± S.E.M. of three determinations.

Measurement of cAMP production

Intracellular cAMP production was determined by measuring the conversion of [^{3}H]ATP to [^{3}H]cAMP, as previously described [46, 47], on cells plated in 35 mm culture dishes. Cells were incubated for 1 h at 37°C with complete culture medium containing 2 µCi/ml of [^{3}H]-adenine. Cells were then washed and incubated for 15 min in 1 mM IBMX in Hank's balanced solution (HBS, pH 7.4) containing 130 mM NaCl, 3.5 mM KCl, 1.8 mM $CaCl_2$, 0.5 mM $MgCl_2$, 2.5 mM $NaHCO_3$, as well as 5 nM HEPES, supplemented with 1 g/L glucose. Following the first incubation, analogs were added to the incubation medium for 15 min at 37°C. Separation of [^{3}H]ATP from [^{3}H]cAMP was obtained by chromatography on Dowex and alumina columns, as described previously [48]. cAMP formation was calculated as follows: % conversion = [^{3}H]cAMP/ ([^{3}H]cAMP + [^{3}H]ATP) x 100/15 min. Inhibition of conversion by the ligand was calculated as follows : % inhibition = ([% $conversion_{sample}$ - % $conversion_{positive\ control}$] / [% $conversion_{\textit{negative control}}$ - % $conversion_{positive\ control}$]) x 100. All analogs were tested at a single concentration of 1 µM, to confirm agonist activity. On selected agonists, EC_{50} was determined by measurements at 10^{-11} to 10^{-6} M. Data were calculated and plotted using Graphpad Prism 5 and represent the mean ± S.E.M. of three determinations.

β-arrestin2 assays

Plasmid expression

β-arrestin2-RlucII expression vector and the fusion vector pIREShygro3-GFP10 were kindly provided by Dr. Michel Bouvier (Dpt of Biochemistry, Université de Montréal). To construct the APJ-GFP10 plasmid, the complete coding sequence of the human apelin receptor was PCR amplified without its stop codon from plasmid template and then fused at C-terminus, in frame to the coding sequence of GFP10 in pIREShygro3 with InFusion advantage PCR cloning kit (Clontech Laboratories, Mountain View, CA) according to the manufacturer's recommendations.

Cell culture and plasmid transfections

Human embryonic kidney (HEK) 293 cells were cultured in high-glucose DMEM supplemented with 10% FBS, 100 U/ ml penicillin-streptomycin, and 2 mM L-glutamine at 37° C in a humidified chamber at 5% CO2. For transient expression of recombinant proteins, 10 cm dishes were seeded with 2,000,000 HEK293 cells. Approximately 18 h later, the cells were transfected using PEI [49].

BRET assays on cells in suspension

For the BRET2-β-arrestin2 recruitment assays, cells co-expressing β-arrestin2-RlucII and APJ-GFP10 were washed once with hank's balanced salt solution (HBSS), detached by gentle pipetting in HBSS, and dispensed into 96-well half area white opaque plates at a density of ~50,000 cells/well. Analogs were added for 20 minutes followed by coelenterazine-400A (5µM final concentration, Biosynth International Inc., Itasca, IL). The BRET2 ratio was determined as emission at 515 nm/400 nm using the BRET2 filters set of the M1000 plate reader (Tecan, Durham, NC). EC_{50} was determined by measurements at 10^{-10} to 10^{-5} M. Data were calculated and plotted using Graphpad Prism 5 and represent the mean ± S.E.M. of three determinations.

Plasma stability

27 µL of rat plasma (obtained from rat blood by keeping the translucent phase after centrifugation at 13000 rpm during 5 min at 4°C) and 6 µL of a 1 mM aqueous solution of analog were incubated at 37°C for 1h, 2h and 3h. The reaction was stopped by adding 70 µL of acetonitrile. After vortexing and centrifugation at 13000 rpm for 20 min at 4°C, the supernatant was analyzed by HPLC-UV (223 nm). To quantify the degradation of analogs, 6 µL of a 1 mM aqueous solution of Fmoc-Glycine was added in each sample as a reference standard just before the HPLC analysis. The

percentage of remaining compound (not degraded) was calculated by doing the ratio between the AUC (area under the curve) of Fmoc-Gly and AUC of the test compound.

REFERENCES

[1] B.F. O'Dowd, M. Heiber, A. Chan, H.H. Heng, L.C. Tsui, J.L. Kennedy, X. Shi, A. Petronis, S.R. George, T. Nguyen, *Gene* **1993**, *136*, 355-360.

[2] K. Tatemoto, M. Hosoya, Y. Habata, R. Fujii, T. Kakegawa, M.X. Zou, Y. Kawamata, S. Fukusumi, S. Hinuma, C. Kitada, T. Kurokawa, H. Onda, M. Fujino, *Biochem. Biophys. Res. Commun.* **1998**, *251*, 471-476.

[3] J. Berta, I. Kenessey, J. Dobos, J. Tovari, W. Klepetko, H. Jan Ankersmit, B. Hegedus, F. Renyi-Vamos, J. Varga, Z. Lorincz, S. Paku, G. Ostoros, A. Rozsas, J. Timar, B. Dome, *J. Thorac. Oncol.* **2010**, *5*, 1120-1129.

[4] L. Bodineau, A. Hus-Citharel, C. Llorens-Cortes, *Ann. Endocrinol. (Paris)* **2010**, *71*, 249-256.

[5] C.J. Charles, *Cardiovasc. Hematol. Agents Med. Chem.* **2007**, *5*, 1-10.

[6] N. De Mota, Z. Lenkei, C. Llorens-Cortes, *Neuroendocrinology* **2000**, 72, 400-407.

[7] N. De Mota, A. Reaux-Le Goazigo, S. El Messari, N. Chartrel, D. Roesch, C. Dujardin, C. Kordon, H. Vaudry, F. Moos, C. Llorens-Cortes, *Proc. Natl. Acad. Sci. U. S. A.* **2004**, *101*, 10464-10469.

[8] C. Dray, C. Debard, J. Jager, E. Disse, D. Daviaud, P. Martin, C. Attane, E. Wanecq, C. Guigne, F. Bost, J.F. Tanti, M. Laville, H. Vidal, P. Valet, I. Castan-Laurell, *Am. J. Physiol. Endocrinol. Metab.* **2010**, *298*, E1161-9.

[9] A.G. Japp, D.E. Newby, *Biochem. Pharmacol.* **2008**, *75*, 1882-1892.

[10] D.K. Lee, S.R. George, B.F. O'Dowd, *Trends Pharmacol. Sci.* **2006**, *27*, 190-194.

[11] A.M. O'Carroll, T.L. Selby, M. Palkovits, S.J. Lolait, *Biochim. Biophys. Acta* **2000**, *1492*, 72-80.

[12] G. Wang, Y. Anini, W. Wei, X. Qi, A.M. OCarroll, T. Mochizuki, H.Q. Wang, M.R. Hellmich, E.W. Englander, G.H. Greeley Jr, *Endocrinology* **2004**, *145*, 1342-1348.

[13] C. Dray, C. Knauf, D. Daviaud, A. Waget, J. Boucher, M. Buleon, P.D. Cani, C. Attane, C. Guigne, C. Carpene, R. Burcelin, I. Castan-Laurell, P. Valet, *Cell. Metab.* **2008**, *8*, 437-445.

[14] Y. Horiuchi, T. Fujii, Y. Kamimura, K. Kawashima, *J. Neuroimmunol.* **2003**, *144*, 46-52.

[15] B. Chandrasekaran, P.R. Kalra, J. Donovan, J. Hooper, J.R. Clague, T.A. McDonagh, *J. Card. Fail.* **2010**, *16*, 556-561.

[16] X.F. Fan, Q. Wang, S.Z. Mao, L.G. Hu, L. Hong, L.X. Tian, Y.Q. Gao, Y.S. Gong, *Zhongguo Ying Yong Sheng Li Xue Za Zhi* **2010**, *26*, 9-12.

[17] M.V. Heinonen, A.K. Purhonen, P. Miettinen, M. Paakkonen, E. Pirinen, E. Alhava, K. Akerman, K.H. Herzig, *Regul. Pept.* **2005**, *130*, 7-13.

[18] A.G. Japp, N.L. Cruden, D.A. Amer, V.K. Li, E.B. Goudie, N.R. Johnston, S. Sharma, I. Neilson, D.J. Webb, I.L. Megson, A.D. Flapan, D.E. Newby, *J. Am. Coll. Cardiol.* **2008**, *52*, 908-913.

[19] D.K. Lee, S.R. George, B.F. O'Dowd, *Trends Pharmacol. Sci.* **2006**, *27*, 190-194.

[20] C. Llorens-Cortes, A. Beaudet, *Med. Sci. (Paris)* **2005**, *21*, 741-746.

[21] Y.P. Visser, F.J. Walther, H. Laghmani el, A. Laarse, G.T. Wagenaar, *Am. J. Respir. Crit. Care Med.* **2010**, *182*, 1239-1250.

[22] N. Xu, H. Wang, L. Fan, Q. Chen, *Peptides* **2009**, *30*, 1153-1157.

[23] X. Fan, N. Zhou, X. Zhang, M. Mukhtar, Z. Lu, J. Fang, G.C. DuBois, R.J. Pomerantz, *Biochemistry* **2003**, *42*, 10163-10168.

[24] X.J. Zeng, L.K. Zhang, H.X. Wang, L.Q. Lu, L.Q. Ma, C.S. Tang, *Peptides* **2009**, *30*, 1144-1152.

[25] S.L. Pitkin, J.J. Maguire, T.I. Bonner, A.P. Davenport, *Pharmacol. Rev.* **2010**, *62*, 331-342.

[26] A.D. Medhurst, C.A. Jennings, M.J. Robbins, R.P. Davis, C. Ellis, K.Y. Winborn, K.W. Lawrie, G. Hervieu, G. Riley, J.E. Bolaky, N.C. Herrity, P. Murdock, J.G. Darker, *J. Neurochem.* **2003**, *84*, 1162-1172.

[27] P. Yue, H. Jin, S. Xu, M. Aillaud, A.C. Deng, J. Azuma, R.K. Kundu, G.M. Reaven, T. Quertermous, P.S. Tsao, *Endocrinology* **2011**, *152*, 59-68.

[28] B. Masri, L. van den Berghe, C. Sorli, B. Knibiehler, Y. Audigier, *J. Soc. Biol.* **2009**, *203*, 171-179.

[29] I. Szokodi, P. Tavi, G. Földes, S. Voutulainen-Myllylä, M. Ilves, H. Tokola, S. Pikkarainen, J. Rysä, M. Tóth, H. Ruskoaho, *Circ. Res.* **2002**, *91*, 434-440.

[30] D.K. Lee, S.S. Ferguson, S.R. George, B.F. O'Dowd, *Biochem. Biophys. Res. Commun.* **2010**, *395*, 185-189.

[31] D.N. Langelaan, E.M. Bebbington, T. Reddy, J.K. Rainey, *Biochemistry* **2009**, *48*, 537-548.

[32] N.J. Macaluso, R.C. Glen, *ChemMedChem* **2010**, *5*, 1247-1253.

[33] N.J. Macaluso, S.L. Pitkin, J.J. Maguire, A.P. Davenport, R.C. Glen, *ChemMedChem* **2011**, *6*, 1017-1023.

[34] J. Hamada, J. Kimura, J. Ishida, T. Kohda, S. Morishita, S. Ichihara, A. Fukamizu, *Int. J. Mol. Med.* **2008**, *22*, 547-552.

[35] X. Iturrioz, R. Alvear-Perez, N. De Mota, C. Franchet, F. Guillier, V. Leroux, H. Dabire, M. Le Jouan, H. Chabane, R. Gerbier, D. Bonnet, A. Berdeaux, B. Maigret, J.L. Galzi, M. Hibert, C. Llorens-Cortes, *FASEB J.* **2010**, *24*, 1506-1517.

[36] X. Iturrioz, R. Gerbier, V. Leroux, R. Alvear-Perez, B. Maigret, C. Llorens-Cortes, *J. Biol. Chem.* **2010**, *285*, 32627-32637.

[37] C. Vickers, P. Hales, V. Kaushik, L. Dick, J. Gavin, J. Tang, K. Godbout, T. Parsons, E. Baronas, F. Hsieh, S. Acton, M. Patane, A. Nichols, P. Tummino, *J. Biol. Chem.* **2002**, *277*, 14838-14843.

[38] K. Janek, J. Behlke, J. Zipper, H. Fabian, Y. Georgalis, M. Beyermann, M. Bienert, E. Krause, *Biochemistry* **1999**, *38*, 8246-8252.

[39] S. El Messari, X. Iturrioz, C. Fassot, N. De Mota, D. Roesch, C. Llorens-Cortes, *J. Neurochem.* **2004**, *90*, 1290-1301.

[40] W. Vogt, *Free Radicals Biol. Med.* **1995**, *18*, 93-105.

[41] C. Ruan, M.T. Rodgers, *J. Am. Chem. Soc.* **2004**, *126*, 14600-14610.

[42] J.E. Robbers, S. Srikrai, H.G. Floss, *J. Nat. Prod.* **1982**, *45*, 178-181.

[43] M. Salomon, A. Jimenez, I. Salazar, R. Zawadzki, *J. Chem. Ed.* **1973**, *50*, 370-371.

[44] C. Wei, D. Tung, Y.M. Yip, Y. Mei, D. Zhang, *J. Chem. Phys.* **2011**, *134*, 171101.

[45] E. Kaiser, R. L. Colescott, C. D. Bossinger, P. I. Cook, *Anal. Bioch.* ***1970,*** *34,* 595.

[46] N. Gallo-Payet, M.D. Payet, *J. Endocrinol.* **1989**, *120*, 409-421.

[47] Z. Kilianova, N. Basora, P. Kilian, M.D. Payet, N. Gallo-Payet, *Endocrinology* **2006**, *147*, 2325-2337.

[48] Y. Salomon, C. Londos, M. Rodbell, *Anal. Biochem.* **1974**, *58*, 541-548.

[49] C. Ehrhardt, M. Schmolke, A. Matzke, A. Knoblauch, C. Will, V. Wixler, S. Ludwig, *Signal Transduction* **2006**, *6*, 179-184.

Table 1

Table 1. Sequence of the D-scan compounds, binding affinity and functional assays.

N°	Sequence	Binding	Functional assays	
		IC_{50} (nM)[a]	EC_{50} cAMP (nM)[b]	cAMP % inhibition at 10^{-5} M[c]
Ape13	<Glu-R-P-R-L-S-H-K-G-P-M-P-F	5.7 ± 0.3	1.89 ± 1	96.0 ± 1.8
1	<Glu-R-P-R-L-S-H-K-G-P-Nle-P-F	2.6 ± 0.3	14.8 ± 5	88.8 ± 1.3
2	<Glu-R-P-R-L-S-H-K-G-P-M-P-***(D)***F	109 ± 16	--	94.8 ± 1.8
3	<Glu-R-P-R-L-S-H-K-G-P-M-***(D)***P-F	44 ± 13	--	89.9 ± 1.3
4	<Glu-R-P-R-L-S-H-K-G-P-***(D)***M-P-F	11 ± 2	--	88.0 ± 0.7
5	<Glu-R-P-R-L-S-H-K-G-***(D)***P-M-P-F	1639 ± 283	--	87.6 ± 0.9
6	<Glu-R-P-R-L-S-H-***(D)***K-G-P-M-P-F	452 ± 119	--	90.0 ± 1.3
7	<Glu-R-P-R-L-S-***(D)***H-K-G-P-M-P-F	305 ± 64	--	89.1 ± 1.6
8	<Glu-R-P-R-L-***(D)***S-H-K-G-P-M-P-F	642 ± 118	--	88.5 ± 1.5
9	<Glu-R-P-R-***(D)***L-S-H-K-G-P-M-P-F	61 ± 10	--	88.6 ± 0.6
10	<Glu-R-P-***(D)***R-L-S-H-K-G-P-M-P-F	1279 ± 271	--	88.4 ± 1.3
11	<Glu-R-***(D)***P-R-L-S-H-K-G-P-M-P-F	3944 ± 545	--	84.4 ± 1.5
12	<Glu-***(D)***R-P-R-L-S-H-K-G-P-M-P-F	4120 ± 672	--	85.5 ± 0.6
13	***(D)***<Glu-R-P-R-L-S-H-K-G-P-M-P-F	26 ± 3	--	90.2 ± 1.4

[a] Concentration producing 50% competitive inhibition of binding of apelin radioligand [^{125}I]-apelin13, values represent the mean ± S.E.M. of three determinations. [b] Concentration producing 50% inhibition of forskolin-induced cAMP accumulation, values represent the mean ± S.E.M. of three determinations. [c] % inhibition of forskolin-induced cAMP accumulation at 10^{-5} M, values represent the mean of three determinations.

This is the accepted version of the following article: Murza, A., et al. (2012), ChemMedChem, 7: 318–325, **which has been published in final form at** http://onlinelibrary.wiley.com/doi/10.1002/cmdc.201100492/abstract

Table 2

Table 2. C-terminal residue substitutions, binding affinity, functional assays and plasma stability.

N°	Sequence	Binding	Functional assays			% remaining after[e]		
		IC_{50} (nM)[a]	EC_{50} cAMP (nM)[b]	cAMP % inhibition at 10^{-5} M[c]	EC_{50} β-arrestin2 (nM)[d]	1h	2h	3h
Ape13	<Glu-R-P-R-L-S-H-K-G-P-M-P-F	5.7 ± 0.3	1.9 ± 1	96.0 ± 1.8	91 ± 17	27	6	0
1	<Glu-R-P-R-L-S-H-K-G-P-Nle-P-F	2.6 ± 0.3	14.8 ± 5	88.8 ± 1.3	--	25	5	0
14	<Glu-R-P-R-L-S-H-K-G-P-Nle-P-**Dip**	88 ± 6	--	93.9 ± 1.9	630 ± 179	71	58	49
15	<Glu-R-P-R-L-S-H-K-G-P-Nle-P-**Bip**	7.8 ± 0.4	10.3 ± 3	88.0 ± 1.4	361 ± 64	67	24	5
16	<Glu-R-P-R-L-S-H-K-G-P-Nle-P-**1Nal**	14.1 ± 0.9	28.6 ± 2	94.4 ± 1.2	522 ± 110	65	59	38
17	<Glu-R-P-R-L-S-H-K-G-P-Nle-P-**2Nal**	1.2 ± 0.1	20.5 ± 6	90.7 ± 2.1	70 ± 11	84	35	6
18	<Glu-R-P-R-L-S-H-K-G-P-Nle-P-**Cha**	2.3 ± 0.6	19.9 ± 8	95.2 ± 0.9	170 ± 32	65	50	30
19	<Glu-R-P-R-L-S-H-K-G-P-Nle-P-**W**	8.5 ± 0.2	--	58.5 ± 1.2	293 ± 64	21	5	0
20	<Glu-R-P-R-L-S-H-K-G-P-Nle-P-**(4-Br)F**	1.2 ± 0.1	12.4 ± 3	90.6 ± 1.6	28 ± 8	47	17	2
21	<Glu-R-P-R-L-S-H-K-G-P-Nle-P-**(2,4,5-trifluoro)F**	0.83 ± 0.2	20.4 ± 9	95.1 ± 2.1	32 ± 9	35	12	5
22	<Glu-R-P-R-L-S-H-K-G-P-Nle-P-**(4-nitro)F**	2.6 ± 0.3	9.8 ± 2	89.4 ± 1.8	53 ± 15	35	15	0

[a] Concentration producing 50% competitive inhibition of binding of apelin radioligand [^{125}I]-apelin13, values represent the mean ± S.E.M. of three determinations. [b] Concentration producing 50% inhibition of forskolin-induced cAMP accumulation, values represent the mean ± S.E.M. of three determinations. [c] % inhibition of forskolin-induced cAMP accumulation at 10^{-5} M, values represent the mean of three determinations. [d] Concentration producing 50% activation of the β-arrestin2 pathway as observed in the BRET assay, values represent the mean ± S.E.M. of three determinations [e] Values represent the mean of two determinations after 1h, 2h and 3h of incubation in rat plasma and are calculated by doing the ratio between surface areas of reference standard Fmoc-Gly and compound signals by HPLC/UV (214 nm).

This is the accepted version of the following article: Murza, A., et al. (2012), ChemMedChem, 7: 318–325, **which has been published in final form at** http://onlinelibrary.wiley.com/doi/10.1002/cmdc.201100492/abstract

Table 3

Table 3. Sequence of the P^{12} substituted compounds, binding affinity, functional assays and plasma stability.

N°	Sequence	Binding	Functional assays			% remaining after[e]		
		IC_{50} (nM)[a]	EC_{50} cAMP (nM)[b]	cAMP % inhibition at 10^{-5} M[c]	EC_{50} β-arrestin2 (nM)[d]	1h	2h	3h
Ape13	<Glu-R-P-R-L-S-H-K-G-P-M-P-F	5.7 ± 0.3	1.89 ± 1	96.0 ± 1.8	91 ± 17	27	6	0
1	<Glu-R-P-R-L-S-H-K-G-P-Nle-P-F	2.6 ± 0.3	14.8 ± 5	88.8 ± 1.3	--	25	5	0
23	<Glu-R-P-R-L-S-H-K-G-P-M-**N_Me_Ala**-F	3.4 ± 0.2	10.0 ± 3	90.1 ± 1.1	114 ± 23	18	0	0
24	<Glu-R-P-R-L-S-H-K-G-P-M-**Aib**-F	0.76 ± 0.1	30.0 ± 13	89.9 ± 1.6	46 ± 10	49	18	12
25	<Glu-R-P-R-L-S-H-K-G-P-M-**HoPro**-F	11.3 ± 2.0	11.6 ± 3	91.5 ± 1.9	453 ± 115	46	12	0
26	<Glu-R-P-R-L-S-H-K-G-P-Nle-**Acpc**-F	2.4 ± 0.4	20.1 ± 4	92.4 ± 0.9	118 ± 23	20	3	0
27	<Glu-R-P-R-L-S-H-K-G-P-Nle-**Aminoindane**-F	20 ± 1.1	--	53.3 ± 1.5	1204 ± 208	57	44	30
28	<Glu-R-P-R-L-S-H-K-G-P-Nle-**cycloleucine**-F	1.6 ± 0.2	--	82.7 ± 0.8	320 ± 43	0	0	0
29	<Glu-R-P-R-L-S-H-K-G-P-Nle-**Aib**-F	1.8 ± 0.2	20.9 ± 7	89.8 ± 1.4	34 ± 7	45	13	6
30	<Glu-R-P-R-L-S-H-K-G-P-Nle-**Inp**-F	5.0 ± 0.9	--	88.5 ± 1.5	42 ± 8	47	32	31
31	<Glu-R-P-R-L-S-H-K-G-P-Nle-**Tle**-F	15.6 ± 2.0	--	73.0 ± 1.1	95 ± 19	61	38	26
32	<Glu-R-P-R-L-S-H-K-G-P-Nle-**Aib-2Nal**	3.6 ± 1.0	12.3 ± 3	91.1 ± 1.9	38 ± 7	24	14	7
33	**Ac-**P-R-L-S-H-K-G-P-Nle-**Aib-2Nal**	2928 ± 766	--	88.4 ± 1.4	>4000	0	0	0
34	**Ac-**R-L-S-H-K-G-P-Nle-**Aib-2Nal**	3453 ± 989	--	92.6 ± 1.4	>3000	0	0	0

[a] Concentration producing 50% competitive inhibition of binding of apelin radioligand [^{125}I]-apelin13, values represent the mean ± S.E.M. of three determinations. [b] Concentration producing 50% inhibition of forskolin-induced cAMP accumulation, values represent the mean ± S.E.M. of three determinations. [c] % inhibition of forskolin-induced cAMP accumulation at 10^{-5} M, values represent the mean of three determinations. [d] Concentration producing 50% activation of the β-arrestin2 pathway as observed in the BRET assay, values represent the mean ± S.E.M. of three determinations. [e] Values represent the mean of two determinations after 1h, 2h and 3h of incubation in rat plasma and are calculated by doing the ratio between surface areas of reference standard Fmoc-Gly and compound signals by HPLC/UV (214 nm).

Table 4

Table 4. Modification of the central portion of the peptide, binding affinity, functional assays and plasma stability.

N°	Sequence	Binding	Functional assays			% remaining after[e]		
		IC_{50} (nM)[a]	EC_{50} cAMP (nM)[b]	cAMP % inhibition at 10^{-6} M[c]	EC_{50} β-arrestin2 (nM)[d]	1h	2h	3h
Ape13	<Glu-R-P-R-L-S-H-K-G-P-M-P-F	5.7 ± 0.3	1.89 ± 1	96.0 ± 1.8	91 ± 17	27	6	0
1	<Glu-R-P-R-L-S-H-K-G-P-Nle-P-F	2.6 ± 0.3	14.8 ± 5	88.8 ± 1.3	--	25	5	0
35	<Glu-R-P-R-L-**$(PEG)_4$**-P-Nle-P-F	450 ± 54	--	9.1 ± 0.7	--	69	25	14
36	<Glu-R-P-R-L-**$(PEG)_6$**-P-F	13700 ± 2066	--	16.7 ± 1.2	--	47	32	25
37	<Glu-R-P-R-L-P-Nle-P-F	5400 ± 889	--	18.9 ± 1.1	--	55	23	8
38	<Glu-R-P-R-L-**A-A-A-A**-P-Nle-P-F	3742 ± 398	--	22.4 ± 0.9	--	42	29	22

[a] Concentration producing 50% competitive inhibition of binding of apelin radioligand [^{125}I]-apelin13, values represent the mean ± S.E.M. of three determinations. [b] Concentration producing 50% inhibition of forskolin-induced cAMP accumulation, values represent the mean ± S.E.M. of three determinations. [c] % inhibition of forskolin-induced cAMP accumulation at 10^{-5} M, values represent the mean of three determinations. [d] Concentration producing 50% activation of the β-arrestin2 pathway as observed in the BRET assay, values represent the mean ± S.E.M. of three determinations. [e] Values represent the mean of two determinations after 1h, 2h and 3h of incubation in rat plasma and are calculated by doing the ratio between surface areas of reference standard Fmoc-Gly and compound signals by HPLC/UV (214 nm).

This is the accepted version of the following article: Murza, A., et al. (2012), ChemMedChem, 7: 318–325, **which has been published in final form at** http://onlinelibrary.wiley.com/doi/10.1002/cmdc.201100492/abstract

Figure 1

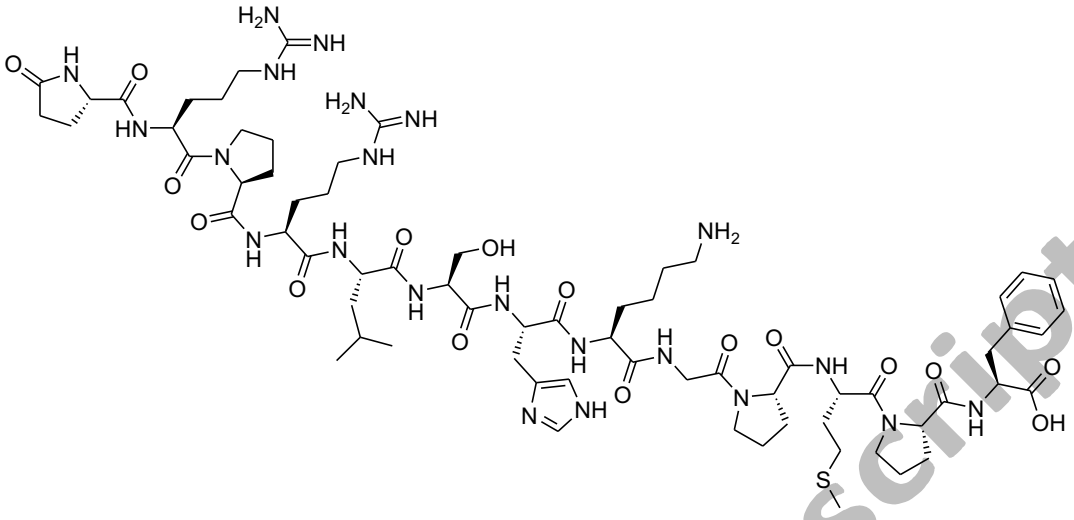

Figure 2

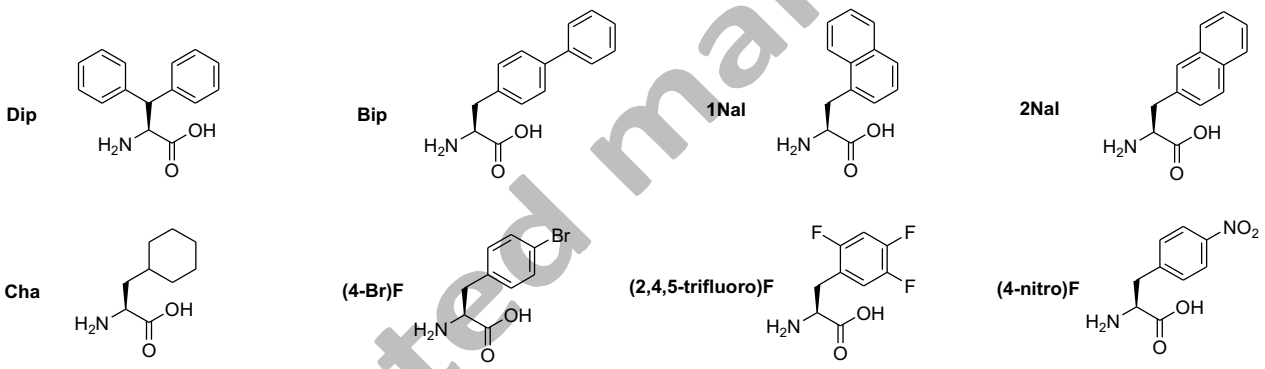

Figure 3